Effect of Stress Type on the Corrosion Behavior of Alloy 600 in Simulated Secondary Water

Byung Joon Bae[a,b], Jeoh Han[a], Jongsup Hong[b], Do Haeng Hur[a*]
[a]*Materials Safety Technology Development Division, Korea Atomic Energy Research Institute, 989-111 Daedeok-daero, Yuseong-gu, Daejeon, 34057, Republic of Korea*
[b]*Division of Mechanical Engineering, Yonsei University, 50 Yonsei-ro Seodaemungu, Seoul, 03722, Republic of Korea*
*Corresponding author: dhhur@kaeri.re.kr

1. Introduction

Alloy 600 steam generator (SG) tubes have been replaced with Alloy 690 because they are well known to be susceptible to corrosion damages such as stress corrosion cracking, and intergranular attack. From extensive studies on secondary side degradation of Alloy 600 SG tubes, it has been verified that corrosion of Alloy 600 is accelerated by impurities [1,2], surface condition [3] and stress [4].

Among these, stress leads to less resistance to corrosion behavior of Ni-based alloys in many aspects. The notable results obtained from numerous studies on effect of stress on corrosion can be followed: an increased crack growth rate [4]; a selective oxidation of chromium [5].

It is noticeable that the corrosion damage by impurities occurs after most surfaces of SG tubes are covered with deposits and oxide layers under diverse stress conditions. However, most of investigations are not considered both stress and oxide layers covering the material before corrosion damage occurs. Therefore, it is necessary to evaluate the characteristics of oxide layer under stress condition.

The objective of this research is to understand the effect of stress type on the oxide layer formation of Alloy 600 SG tube material in simulated secondary water. To achieve this goal, two different stress types of specimen were prepared and corrosion test is performed at 340 ℃ for 1000 h in simulated secondary water.

2. Experimental Methods

2.1. Preparation of Specimens

Every specimen was prepared from Alloy 600 plates, which were mill annealed (MA) at 950 ℃ for 2 h and air cooled to relieve stress. The chemical composition of Alloy 600 is shown in Table 1.

Table. 1. Chemical composition of Alloy 600 (wt. %).

Ni	Cr	Fe	Mn	C	Si	Cu
75.2	15.03	8.23	0.39	0.048	0.08	0.01

Test specimens were used in two different types (U-bend type and plate type). U-bend type specimen is for stressed condition and plate type specimen is for stress-free condition. Before bending, they were ground with silicon carbide papers from #600 grits to #1000 grits to achieve in same surface condition, and then ultrasonically cleaned in acetone. The ground specimens were bent in a U-bend shape according to the guideline provided by ASTM G30-97 as shown in Fig. 1.

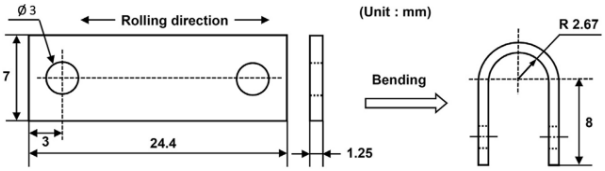

Fig. 1. Dimensions of a U-bend type specimen.

2.2. Corrosion Test

Corrosion test was performed in a secondary water circulating loop system shown in Fig. 2. The test solution was deionized water of which pH was adjusted with ethanolamine to 9.0 at 25 ℃. To eliminate the effect of oxygen, dissolved oxygen of the solution in a feed tank and a pH control tank was controlled to be less than 5 ppb using high purity nitrogen gas. Different two types of specimen were loaded on a specimen holder made of Alloy 600 material to avoid any galvanic corrosion between the specimens and holder. The test solution was circulated the loop system at a flow rate of 200 ml/min and maintained at 340 ℃ under 150 bars for 1000 h.

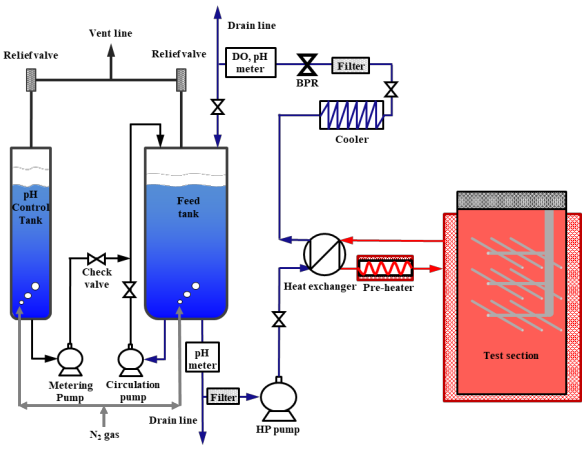

Fig. 2. Schematic of the loop system for the corrosion test.

2.3. Oxide layer Analysis

After the test, the morphology of oxide layers and particles formed on the specimens was observed using a scanning electron microscope (SEM). The focused ion beam milling technique was used to produce samples for a transmission electron microscope (TEM). For the specimens under the tensile stress condition, TEM samples were produced at the apex of the U-bend specimens, where the strain of specimen was the maximum. The distribution of chemical species was analyzed by using line and mapping analyses of an energy dispersive X-ray spectroscopy (EDS) attached to the TEM.

3. Result and Discussion

Fig. 3 shows the SEM micrographs on the morphologies of the outer oxide films formed on Alloy 600 MA. The surface morphologies of outer oxide films between tensile stress condition and stress-free condition were significantly different. Under both the conditions, the outer oxide films were covered with numerous polyhedral oxide particles mostly. However, as shown in Fig. 3 (a), oxide particles with diameter of larger than 1 μm were observed more frequently on the specimen under the tensile stress condition compared with under the stress-free condition.

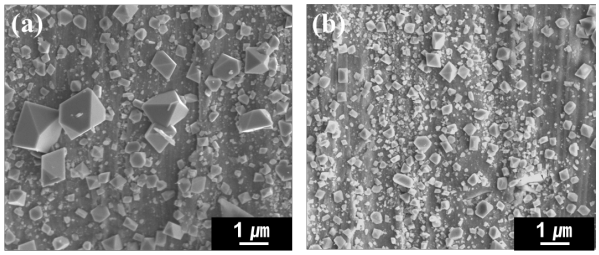

Fig. 3. SEM images of specimens after 1000 h corrosion test: (a) tensile stress condition, (b) stress-free condition.

Fig. 4 shows the STEM-EDS mapping image of the oxide layer formed under the tensile stress condition and stress-free condition. In both the conditions, oxide particles on the outer surface were composed of nickel and iron in major. However, the inner oxide layer formed under the tensile stress condition was thicker than that formed under the stress-free condition. The larger particles and the thicker oxide layer indicate that the corrosion rate of the tensile-stressed specimen was higher than that of the stress-free specimen.

Fig. 5 shows STEM images and EDS line profiles of Cr, Fe and Ni across the oxide layers after the corrosion test. The location and direction of the measurement are denoted with a white arrow. As shown in Fig. 5, the outside oxide particles formed under both the conditions were composed of nickel and iron. There was no dramatic difference in the thickness of Cr-rich inner layers and Cr-depleted inner layers under the both stress conditions. However, the chromium content in the Cr-rich oxide layer under the stress-free condition was approximately 80 wt. %, significantly higher than about 20 wt. % under the tensile stress condition.

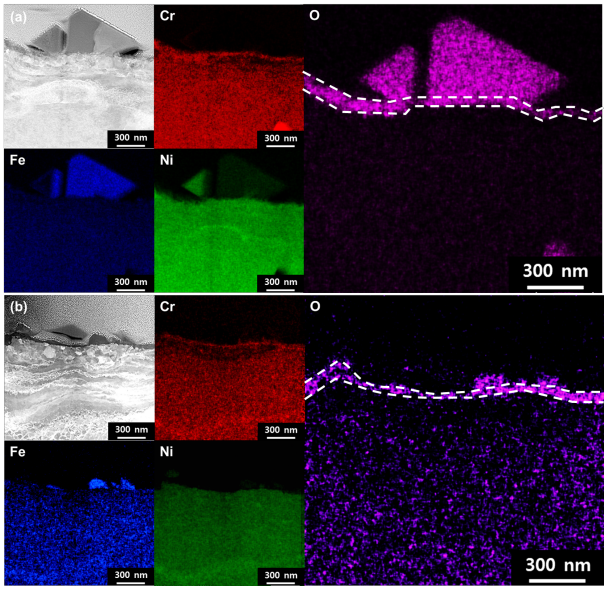

Fig. 4. STEM-EDS mapping image of specimens after 1000 h corrosion test: (a) tensile stress condition, (b) stress-free condition.

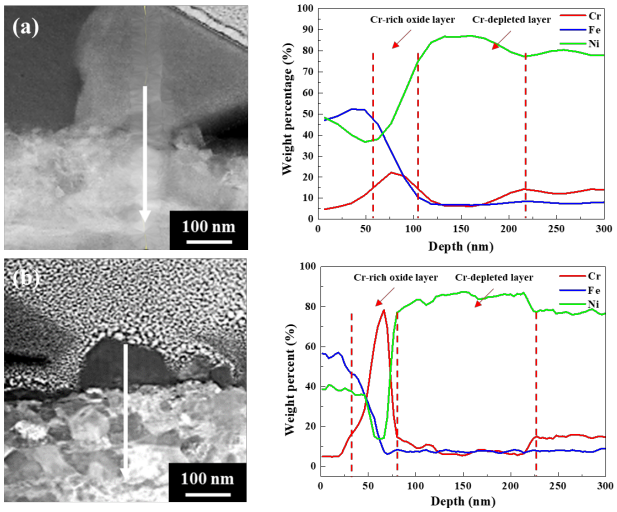

Fig. 5. STEM images and EDS line profiles on the outer oxide film of specimens after 1000 h corrosion test: (a) tensile stress condition, (b) stress-free condition.

Chromium is well known as a resistant component to corrosion and directly related to corrosion and stress corrosion cracking behavior of stainless steels and N-based alloys [6,7]. Thus the lower chromium content of the inner oxide layer formed under the tensile stress condition could affect the corrosion and stress corrosion cracking of Ni-based alloys.

4. Conclusions

1) Oxide particles on the outer surface were polyhedral nickel ferrite in general. However, the oxide particles with diameter of lager than 1 μm were observed relatively more under the tensile

stress condition.

2) The inner oxide layer formed under the tensile stress condition was thicker than that formed under the stress-free condition.

3) The chromium content in the Cr-rich oxide layer under the tensile stress condition was only 20 wt. %, compared to 80 wt. % under the stress-free condition. Therefore, a rapid stress corrosion cracking of Alloy 600 under tensile stress can be attributed to the relative low chromium content in the inner oxide layer.

Acknowledgements

This work was supported by the National Research Foundation (NRF) grant funded by the government of the Republic of Korea (NRF-2017M2A8A4015159).

REFERENCES

[1] B.T. Lu, J.L. Luo, Y.C. Lu, Passivity Degradation of Nuclear Steam Generator Tubing Alloy induced by Pb Contamination at High Temperature, Journal of Nuclear Materials, Vol.429, p305, 2012.
[2] D.H. Hur, M.S. Choi, D.H. Lee, M.H. Song, J.H. Han, Root Causes of Intergranular Attack in an Operating Nuclear Steam Generator Tube, Journal of Nuclear Material. Vol.375, p382, 2008.
[3] W.I. Choi, G.D. Song, S.H. Jeon, S.J. Kim, D.H. Hur, Magnetite-Accelerated Stress Corrosion Cracking of Alloy 600 in Water containing 100ppm Lead Oxide at 315 ℃, Journal of Nuclear Materials, Vol.522, p54, 2019.
[4] R.B. Rebak, Z. Szklarska-Smialowska, The Mechanism of Stress Corrosion Cracking of Alloy 600 in High Temperature Water, Corrosion Science, Vol.38, p971, 1996.
[5] G. Bertali, F.Scenini, M.G. Burke, The Effect of Residual Stress on the Preferential Intergranular Oxidation of Alloy 600, Corrosion Science, Vol.111, p. 494, 2016.
[6] T. Terachi, T. Yamada, T. Miyamoto, K. Arioka, K. Fukuya, Corrosion Behavior of Stainless Steels in Simulated PWR Primary Water-Effect of Chromium Content in Alloys and Dissolved Hydrogen, Journal of Nuclear Science and Technology, Vol.45, p.975, 2008.
[7] F. Delabrouille, B. Viguier, L. Legras, E. Andrieu, Effect of the Chromium Content on the Corrosion of Nickel based Alloys in Primary Water of Pressurised Nuclear Reactors, Materials at High Temperatures, Vol.22, p287, 2005.